

# Conceptual framework for model-based analysis of residence time distribution in twin-screw granulation

Ashish Kumar<sup>a,b</sup>, Jurgen Vercruysse<sup>c</sup>, Valérie Vanhoorne<sup>c</sup>, Maunu Toiviainen<sup>d</sup>, Pierre-Emmanuel Panouillot<sup>d</sup>, Mikko Juuti<sup>d</sup>, Chris Vervaet<sup>c</sup>, Jean Paul Remon<sup>c</sup>, Krist V. Gernaey<sup>e</sup>, Thomas De Beer<sup>b,1</sup>, Ingmar Nopens<sup>a,\*</sup>

<sup>a</sup>*BIOMATH, Department of Mathematical Modelling, Statistics and Bioinformatics, Faculty of Bioscience Engineering, Ghent University, Coupure Links 653, B- 9000 Gent, Belgium*

<sup>b</sup>*Laboratory of Pharmaceutical Process Analytical Technology, Department of Pharmaceutical Analysis, Faculty of Pharmaceutical Sciences, Ghent University, Harelbekestraat 72, B-9000 Ghent, Belgium*

<sup>c</sup>*Laboratory of Pharmaceutical Technology, Department of Pharmaceutics, Faculty of Pharmaceutical Sciences, Ghent University, Harelbekestraat 72, B-9000 Ghent, Belgium*

<sup>d</sup>*Optical Measurement Technologies, VTT Technical Research Centre, Kuopio, Finland*

<sup>e</sup>*CAPEC-PROCESS, Department of Chemical and Biochemical Engineering, Technical University of Denmark, 2800 Kongens Lyngby, Denmark*

---

\*Email address: [ingmar.nopens@ugent.be](mailto:ingmar.nopens@ugent.be), Tel.: +32 (0)9 264 61 96; fax: +32 (0)9 264 62 20

*Email addresses:* [ashish.kumar@ugent.be](mailto:ashish.kumar@ugent.be) (Ashish Kumar), [jurgen.vercruysse@ugent.be](mailto:jurgen.vercruysse@ugent.be) (Jurgen Vercruysse), [valerie.vanhoorne@ugent.be](mailto:valerie.vanhoorne@ugent.be) (Valérie Vanhoorne), [maunu.toiviainen@vtt.fi](mailto:maunu.toiviainen@vtt.fi) (Maunu Toiviainen), [pierre-emmanuel.panouillot@vtt.fi](mailto:pierre-emmanuel.panouillot@vtt.fi) (Pierre-Emmanuel Panouillot), [mikko.juuti@vtt.fi](mailto:mikko.juuti@vtt.fi) (Mikko Juuti), [chris.vervaet@ugent.be](mailto:chris.vervaet@ugent.be) (Chris Vervaet), [jeanpaul.remon@ugent.be](mailto:jeanpaul.remon@ugent.be) (Jean Paul Remon), [kvg@kt.dtu.dk](mailto:kvg@kt.dtu.dk) (Krist V. Gernaey), [thomas.debeer@ugent.be](mailto:thomas.debeer@ugent.be) (Thomas De Beer)

*URL:* [www.biomath.ugent.be](http://www.biomath.ugent.be) (Ingmar Nopens)

<sup>1</sup>Shared last authorship

## 1 **Abstract**

2 Twin-screw granulation is a promising continuous alternative for traditional batchwise  
3 wet granulation processes. The twin-screw granulator (TSG) screws consist of transport and  
4 kneading element modules. Therefore, the granulation to a large extent is governed by the  
5 residence time distribution within each module where different granulation rate processes  
6 dominate over others. Currently, experimental data is used to determine the residence time  
7 distributions. In this study, a conceptual model based on classical chemical engineering  
8 methods is proposed to better understand and simulate the residence time distribution in  
9 a TSG. The experimental data were compared with the proposed most suitable conceptual  
10 model to estimate the parameters of the model and to analyse and predict the effects of  
11 changes in number of kneading discs and their stagger angle, screw speed and powder feed  
12 rate on residence time. The study established that the kneading block in the screw con-  
13 figuration acts as a plug-flow zone inside the granulator. Furthermore, it was found that a  
14 balance between the throughput force and conveying rate is required to obtain a good axial  
15 mixing inside the twin-screw granulator. Although the granulation behaviour is different  
16 for other excipients, the experimental data collection and modelling methods applied in this  
17 study are generic and can be adapted to other excipients.

18 *Keywords:* Residence time distribution, flow modelling, axial mixing, stagnant zone, wet  
19 granulation

## 1. Introduction

Traditionally, granulation is performed in batch mode. However, a supportive regulatory environment and process economics are driving the switch towards continuous manufacturing. In this context, twin-screw granulation is emerging as a potential continuous granulation technique. In a twin-screw granulator (TSG) featuring short residence times, mixing of powder and liquid phase and particle enlargement is achieved by the modular/interchangeable configuration of the screw design. The granule size distribution (GSD) is governed by the complex relationship between principal rate processes such as wetting, nucleation, agglomeration, breakage and consolidation (Dhenge et al., 2012; Kumar et al., 2014a), each of which can dominate over others based on the local environment within each module such as degree of mixing and free surface liquid for further granulation. Mixing in these modules of the TSG results from kinematic processes described in terms of displacement (caused by incoming flow) and drag (direct parameters from vectorised fields) flows. The ratio of these flows is related to the screw configuration and the operating conditions of the TSG resulting into different filling degrees and residence time distributions (RTDs).

Changes in screw geometry and operating parameters influence both the mean residence time ( $\bar{t}$ ) and the width of the RTD given by the mean centered variance ( $\sigma_{t_m}^2$ ) (Kumar et al., 2014b). While the radial mixing by the kneading blocks inside the TSG is related to the  $\bar{t}$ , the longitudinal or axial mixing performance is determined by the  $\sigma_{t_m}^2$ . Narrow RTDs lead to a uniform product and are generally considered to be favourable. However, axial mixing in addition to the radial mixing is equally required in the TSG to avoid the effect of any inhomogeneities (such as the ones caused by non-optimal performance of the pre-blender and periodicity of the feeders and pumps) at the inlet on the produced granules (Kumar et al., 2014b).

Due to the difficulties to visualise the material flow in the barrel, little efforts have been made thus far towards understanding the RTD and mixing of material inside the TSG barrel. Dhenge et al. (2010) measured the RTD using the impulse-response technique under different processing conditions and showed that the variation in the RTD depends on formulation and

48 process parameters. El Hagrasy et al. (2013) applied the same RTD measurement approach  
49 to estimate the response to changes in formulation properties such as raw material attributes  
50 as well as granulation liquid properties on granule properties. In a recent attempt, Lee et al.  
51 (2012) obtained the RTD using positron emission particle tracking (PEPT) and concluded  
52 that the extent of axial mixing was the same for different screw geometries. Although  
53 PEPT is a very powerful measurement technique, such a conclusion can also arise due to the  
54 inability of the circulated PEPT tracers to provide information on the total flow behaviour  
55 as some material paths occur rarely, and are hence not followed by the finite number of tracer  
56 paths through the equipment. Therefore, only distributions of passage time rather than a  
57 true RTD can be measured using PEPT (Bakalis et al., 2004). Kumar et al. (2014b) applied  
58 near infrared chemical imaging (NIR-CI) to measure the RTD to conclude that the extent of  
59 axial mixing is significantly influenced by the screw configuration and barrel filling degree.  
60 The adequateness of the NIR-CI as an analytical tool for the visualization of the process  
61 in a TSG requiring fast measurements was established in an earlier study by Vercruyse  
62 et al. (2013). In this study on granulation liquid mixing and distribution along with the  
63 residence time analysis in TSG it was concluded that the liquid distribution improved only  
64 by increasing the granulation liquid content at the granulator inlet.

65 As for experimental process visualisation, the efforts toward predictive modelling of the  
66 RTD in TSG are sparse compared to other fields employing extrusion based systems, such as  
67 the food and polymer industries (Gao et al., 2012). This is mainly due to the difficulties in  
68 defining the intrinsic physico-chemical properties of the formulation mixture in the opaque  
69 and high-shear process environment of the TSG (Kumar et al., 2013a). Therefore, local mass  
70 balances are complex to be solved, hence requiring drastically simplified hypotheses. Kumar  
71 et al. (2013b) presented a one-dimensional transport model based on screw geometry and  
72 material characteristics. However, conceptual flow modelling is another approach, in which  
73 the transport process is modelled as a combination of ideal reactors, the plug-flow reactor  
74 (PFR) having no axial mixing and the constantly stirred tank reactors ( $n$ ) having perfect  
75 axial mixing. Originally derived for chemical reactors, different types of single and multi-  
76 stage models and their applications have been widely discussed in the literature (Levenspiel,

1999; Puaux et al., 2000; Fogler, 2006; Kumar et al., 2008). For a non-ideal flow system like the TSG, the conceptual model used for RTD modelling generally consists of combinations of plug-flow volume fraction ( $p$ ), a finite number of  $n$  with stagnant pockets or dead zones ( $d$ ) to closely represent the flow pattern. This approach was also adopted by Lee (2013) to explain the experimental RTDs obtained from PEPT measurements in a continuous TSG.

However, to our best knowledge, a systematic evaluation of the performances of different conceptual models for their ability to describe flow and transport in a TSG for a broad spectrum of process conditions is still not available. Therefore, the objective of this study was to compare some of the existing conceptual models based on goodness-of-fit between the calibrated model and the experimental data, in order to identify the most suitable model configuration for describing the RTD in a TSG. Furthermore, the effect of input variables, screw configuration (number and stagger angle of kneading discs) and fill ratio (governed by screw speed and powder feed rate), was analysed by simulating the calibrated model.

## 2. System analysis and model formulation

### 2.1. Continuous wet-granulation using TSG

The TSG consists of a barrel enclosing two co-rotating self-wiping screws. At the entrance, raw materials are fed into the transport zone and the granulation liquid is added via two nozzles, one for each screw, before the material reaches the mixing zone which consists of kneading discs (Fig. 1). The modular structure of the screws allows changing the number of kneading discs, hence the length of the mixing zone. The powder is hence wetted by the granulation liquid in this region. Further down, since the granulation occurs by a combination of capillary and viscous forces binding particles in the wet state, the wetted material is distributed, compacted and elongated by the kneading discs of the mixing zones, changing the particle morphology from small (microstructure) to large (macrostructure). It is believed that the material is mixed, compacted and chopped to form irregular and porous granules by the succeeding transport elements and kneading blocks (Vercruyssen et al., 2012). The rotation of the screws conveys the material in axial direction through the different zones

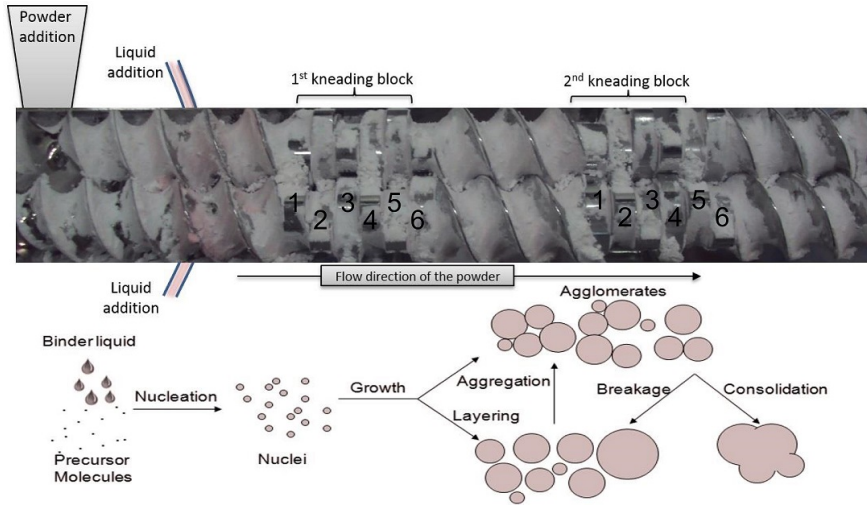


Figure 1: Screw configuration with 12 kneading discs (2 blocks containing 6 kneading discs each) indicating the geometry and flow of material inside the TSG barrel.

104 of the TSG by the drag and flow-induced displacement forces and thus causing mixing and  
 105 granulation. The rheological behaviour of the material also changes based on liquid-to-solid  
 106 ratio (L/S) (Althaus and Windhab, 2012).

## 107 2.2. Experimental determination of RTD

108 The RTD experimental data for the twin-screw granulation were obtained using a 25 mm  
 109 diameter co-rotating twin screw granulator, which is the granulation module of the ConsiGma-  
 110 25 unit (GEA Pharma Systems, Collette™, Wommelgem, Belgium). The granulator screw  
 111 has a length-to-diameter ratio of 20:1. The barrel jacket was preheated to 25°C. During  
 112 processing, pure  $\alpha$ -lactose monohydrate was gravimetrically fed into the granulator by us-  
 113 ing a twin-screw feeder (KT20, K-Tron Soder, Niederlenz, Switzerland). The granulation  
 114 liquid was added (11.5% w/w) before the first kneading element by dripping through two  
 115 liquid feed ports (Fig. 1). Each port was located on the central top of each screw in the  
 116 barrel. Experimental RTDs were obtained by spiking anhydrous theophylline (2% (w/w)  
 117 of the actual throughput (g/min)) into the powder inlet port of the granulator. The TSG  
 118 has an inbuilt torque gauge and the criterion indicating steady state was decided based on  
 119 the equilibration of the measured torque of the granulator. Spectral images of wet gran-  
 120 ules were collected using a line-scanning (pushbroom) hyperspectral camera (SWIR, Specim

121 Ltd., Oulu, Finland). The spatial distribution of theophylline was measured during the first  
 122 25 seconds following tracer addition using the spectral matched filter method. Details of  
 123 the experimental set-up, procedure and DoE have been described earlier by Kumar et al.  
 124 (2014b).

### 125 2.3. Estimation of RTD from experimental data

126 A RTD was derived by injecting a pulse of tracer into the system at the inlet, and the  
 127 residence time function,  $e(t)$ , was calculated as

$$e(t) = \frac{c(t)}{\int_0^\infty c(t)dt} \quad (1)$$

128 where  $c(t)dt$  is the concentration of the tracer at the outlet between time points  $t$  and  $t + dt$ .

129 This tracer map was then transformed into the exit age distribution curve, i.e. the RTD  
 130 based on the mean tracer concentration,  $e(t)$  between  $t$  and  $t + dt$ , which was then used to  
 131 calculate the mean residence time ( $\bar{t}$ ) as the ratio of the first and the zeroth moment using  
 132 equation

$$\bar{t} = \frac{\int_0^\infty t.e(t)dt}{\int_0^\infty e(t)dt} \quad (2)$$

133 The RTD shape and  $\bar{t}$  thus obtained were used to obtain the normalised residence time  
 134 as  $e(\theta) = \bar{t}.e(t)$ , where dimensionless time,  $\theta = t/\bar{t}$ .

### 135 2.4. Theoretical models for RTD in TSG

136 In the previous experimental studies, the RTDs obtained for TSG showed intermedi-  
 137 ate flow characteristics between the two ideal cases, the perfectly-mixed flow and the plug  
 138 flow (Lee et al., 2012; Kumar et al., 2014b). Therefore, models for non-ideal flow have to  
 139 be used to describe the material flow inside the TSG. Major considerations for the selection  
 140 of a flow model are, the physical significance of the model and the number of adjustable  
 141 parameters.

142 In order to have a physical significance, the model structure should be able to characterise  
 143 the real process through its parameters. In this study, three model candidates were selected

144 to simulate the RTD of the twin-screw granulator: the tanks-in-series (TIS) model without  
 145 a plug-flow volume fraction, the TIS with a plug-flow volume fraction and the TIS including  
 146 a plug-flow volume fraction and dead zones (Fig. 2). The TIS model without a plug-flow  
 147 volume fraction is a one-parameter flow model expressed as (Levenspiel, 1999)

$$e(\theta) = \frac{n(n\theta)^{n-1}}{(n-1)!} \exp(-n\theta) \quad (3)$$

148 where,  $n$  is the constantly stirred tank reactors. The closer the  $n$  value to unity, the higher  
 149 the degree of mixing, and vice-versa. The TIS model containing a plug-flow volume fraction  
 150 as well is a three-parameter flow model given by (Levenspiel, 1999)

$$e(\theta) = \frac{b[b(\theta - p)]^{n-1}}{(n-1)!} \exp[-b(\theta - p)] \quad (4)$$

where,  $p = \frac{t_{min}}{\bar{t}}$  and,  $b = \frac{n}{1-p}$

151 where,  $t_{min}$  is the minimum residence time and  $p$  is the fraction of the volume of the TSG  
 152 that is assumed to correspond to the plug-flow volume fraction. For the TIS model with  
 153 both plug-flow volume fraction and dead zones, which is a four-parameter flow model, the  
 154 calculation of  $e(\theta)$  and the  $p$  in eq. 4 remains the same, whereas the  $b$  is modified as (Kumar  
 155 et al., 2008)

$$b = \frac{n}{(1-p)(1-d)} \quad (5)$$

156 where,  $d$  is the dead zone of continuously-stirred tank reactors indicating the fraction of  
 157 material which is either excessively back-mixed or spend much longer time than  $\bar{t}$  in the  
 158 stagnant pockets that exist in the TSG. Normally, this material spends more than twice the  
 159  $\bar{t}$ , and the average velocity is much smaller compared to the well mixed region, leading to a  
 160 long tail in the RTD. Hence, the four parameters that are present in these models are  $\bar{t}$ ,  $n$ ,  
 161  $p$  and  $d$ . tendency for

162 Regarding the number of adjustable parameters, the heuristic rule is to use the model



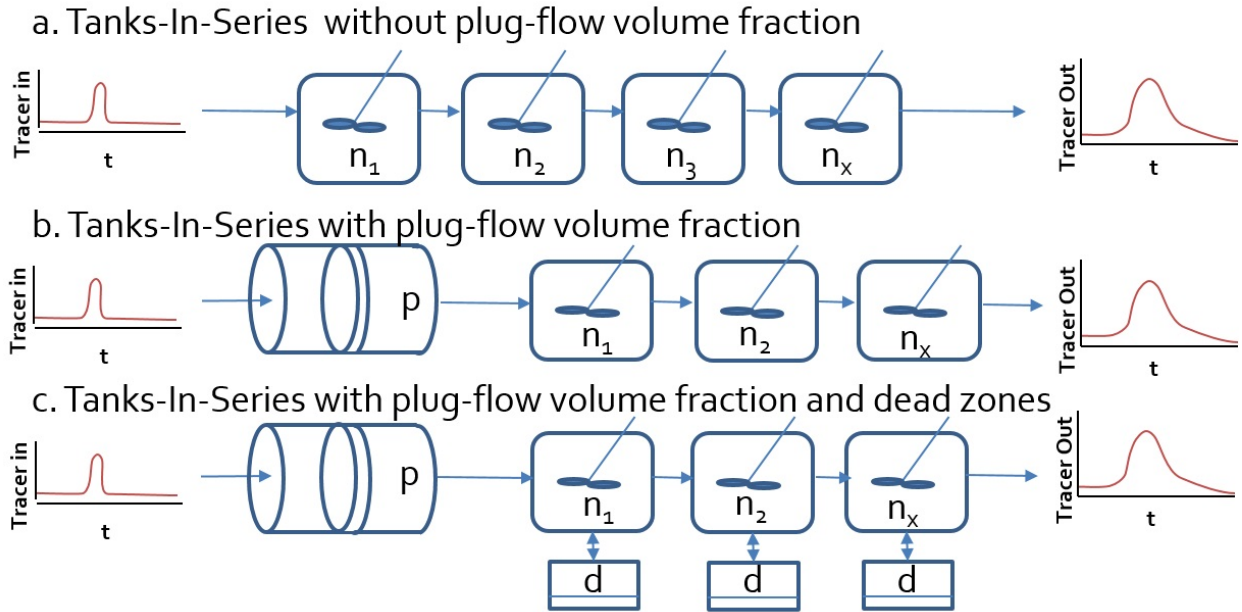


Figure 2: Schematic diagram of three conceptual models based on non-ideal flow for the RTD in a TSG with a series of continuously stirred tank reactors (a) without a plug-flow volume fraction , (b) with a plug-flow volume fraction , and (c) with plug-flow volume fraction and dead zones.

163 with the lowest number of parameters. Since the TIS model with both plug-flow volume  
 164 fraction and dead zones contained four adjustable parameters, practical identifiability was  
 165 studied in order to verify the reliability of parameter estimates and their functional relation.  
 166 The collinearity analysis was used to detect practical identifiability problems over the com-  
 167 plete parameter space  $\mathbf{S}$ . Columns of a matrix  $\mathbf{S}$  are called near collinear if there exists a  
 168 vector  $\beta$  such that  $\|\beta\| \neq 0$  and  $S\beta \approx 0$ . The collinearity among columns  $\mathbf{S}_k= 1, 2, \dots, m$ , of  
 169  $\mathbf{S}$  was tested by inspecting the smallest eigenvalue  $\lambda_m$  of the normalised sensitivity matrix,  
 170  $\tilde{\mathbf{S}}$ . For details see Brun et al. (2001). Finally, the collinearity index,  $\gamma$  was calculated as

$$\gamma = \frac{1}{\min_{\|\beta\|=1} \|\tilde{\mathbf{S}}\beta\|} = \frac{1}{\sqrt{\lambda_m}} \quad (6)$$

171 A high collinearity index indicates correlation among the parameters. Parameter subsets  
 172 with collinearity index smaller than 5 are considered as identifiable and collinearity index  
 173 values above 20 are considered non-identifiable (Brun et al., 2001).

174 *2.5. Parameter estimation*

175  $\bar{t}$  and  $p$  were estimated from the RTD measurement data using eqs. 2 and 4 respectively.  
176 The estimation of the other two parameters of different TIS models,  $n$  and  $d$  was done using  
177 the residual sum of squares (RSS) as an objective function (eq. 7), which was minimised. In  
178 order to find the global minimum of the objective function, the "brute force" method was  
179 used, which computes the objective function's value at each point of a multidimensional  
180 grid of points, to arrive at the global minimum of the function. This multidimensional grid  
181 contained ranges of  $n$  (1 to 10),  $p$  (0 to 0.75) and  $d$  (0 to 0.75) with linear step length of 1,  
182 0.005 and 0.005, respectively. Later, to obtain a more precise (local) minimum near brute's  
183 best gridpoint, the downhill simplex algorithm was used applying the result of "brute force"  
184 minimization as initial guess (Nelder and Mead, 1965).

$$\text{RSS} = \sum (e(\theta)_{\text{exp}} - e(\theta)_{\text{sim}})^2 \quad (7)$$

185 *2.6. Model analysis*

186 The RSS values were obtained by comparing experimental data,  $e(\theta)_{\text{exp}}$  with the simu-  
187 lated data,  $e(\theta)_{\text{sim}}$  of the conceptual models presented in section 2.4 (Fig. 3, 4, eq. 7). Two  
188 different techniques are used to find if the model is adequate to describe the RTD and hence  
189 transport and mixing inside the TSG. First, the coefficient of determination ( $R^2$ ) was used,  
190 which is a statistical measure of how well the simulated data points approximate the real  
191 measurement data points. Acceptable values of  $R^2$  (close to 1) imply that the respective  
192 model defines the true behaviour of the system. Second, RSS was used which is a measure  
193 of the discrepancy between the experimental data and an estimation model. A small RSS  
194 indicates a close fit of the model to the data.

195 The calculations for parameter estimation and model analysis were performed using the  
196 Python programming language, employing built-in functions in scientific libraries NumPy  
197 and SciPy (Oliphant, 2007). If a conceptual framework for RTD could demonstrate a high  $R^2$   
198 value and RSS for a broad spectrum of process conditions, this would form a strong indication  
199 that the model is suitable and thus can be used for interpolation in the experimental domain.

### 200 3. Results and Discussion

#### 201 3.1. Comparison of models based on the goodness-of-fit

##### 202 *Tanks-in-series (TIS)*

203 This model allowed estimation of the axial mixing of the bulk material stream under a  
204 non-ideal mixing condition in terms of  $n$  (eq. 3) (Levenspiel, 1999). The RSS between the  
205 experimental data and the model prediction was calculated for the  $n$  values ranging from  
206 1–50. The parameter  $n$  that gave the least RSS varied from 2 to 30 for the different runs  
207 (Fig. 3). The  $n$  increased with an increase in  $\bar{t}$ . An increase in number and stagger angle of  
208 kneading discs and a reduction in screw speed led to an increase in the  $\bar{t}$ . However, there  
209 was a significant lack of fit obtained for this model as the  $R^2$  for the different runs for this  
210 model varied from 0.50–0.94. Also, the RSS was found to be between 54–265. This suggests  
211 that this model structure was not suitable to conceptually describe the RTD in the TSG.  
212 The high value of  $n$  estimated by this model also indicates that axial mixing in the TSG  
213 was non-ideal. Therefore, in order to improve accuracy in simulating the flow behaviour of  
214 the material in the TSG, a plug-flow volume fraction was needed to be introduced in the  
215 TIS model (eq. 4). In lack of axial mixing, the flow in a plug-flow volume fraction rely on  
216 the conveying rate only. Hence, it is a cause of delay in the appearance of the tracer in the  
217 outlet.

##### 218 *TIS with plug-flow volume fraction*

219 This model structure contained two physically significant parameters ( $p$  and  $n$ ) thus  
220 allowing the quantification of the plug-flow volume fraction along with the degree of mixing,  
221 respectively. As for the TIS without a plug-flow volume fraction, the estimated parameters  
222 of the TIS with a plug-flow volume fraction also suggest a deviation from the ideal-plug and  
223 mixed flow behaviour in the TSG. Including the  $p$  as model component caused a significant  
224 reduction in the value of  $n$ , which now ranged between 2–21. The value of  $p$  for different runs  
225 were obtained between 0.2–0.65. The existence of a plug-flow regime was clearly identified by  
226 this model, and resulted in a lower RSS and higher  $R^2$  ranges compared to the TIS without a  
227 plug-flow volume fraction. The RSS and the  $R^2$  were obtained between 42–305 and 0.73–0.97,

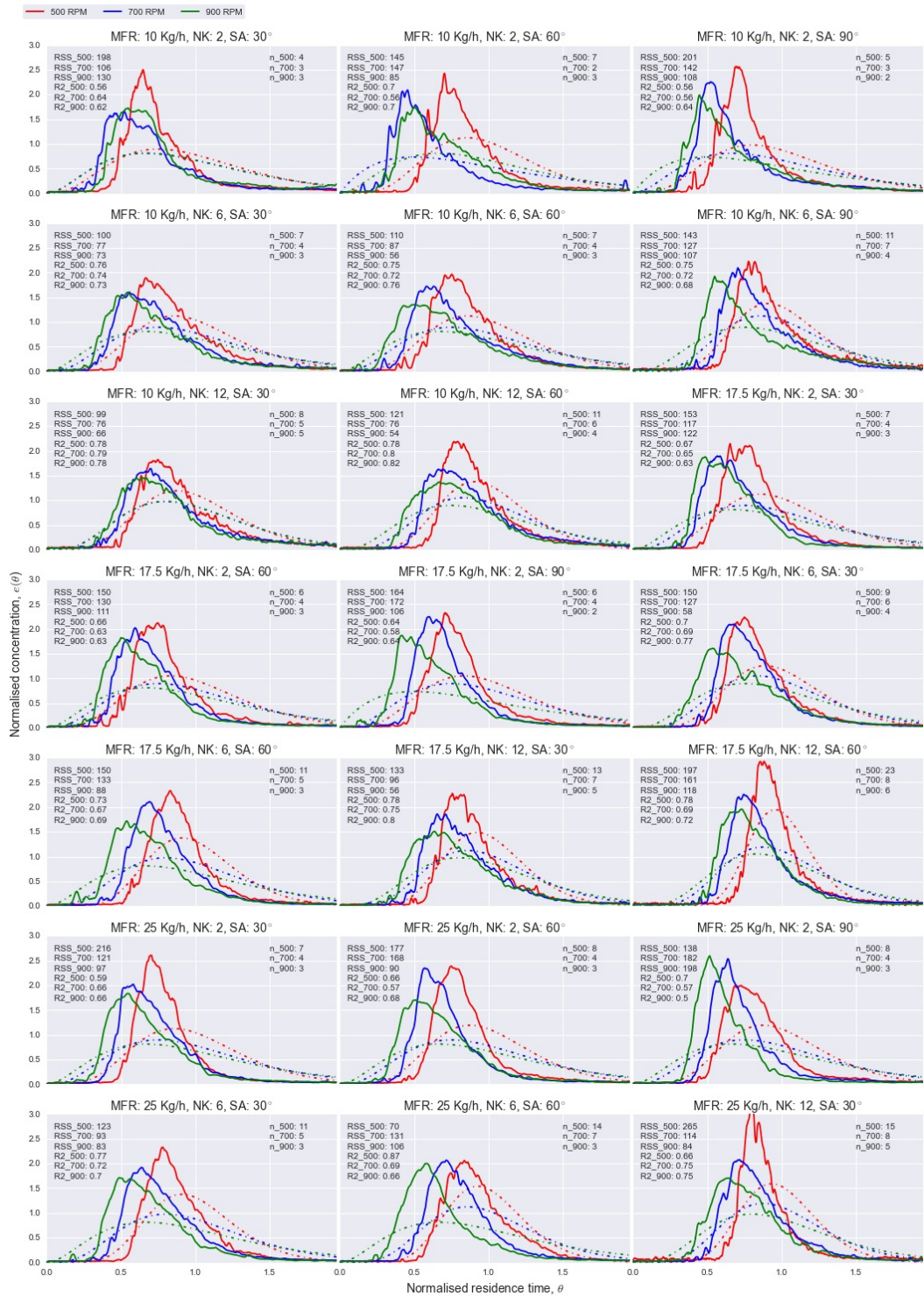


Figure 3: Experimental (—) vs. predicted (---) RTD by a TIS model at different screw speed (500, 700, 900 RPM), powder feed rate (10-25 kg/h), number of kneading discs (2, 6, 12) and stagger angle (30-90°) [SA: stagger angle (°), NK: number of kneading discs (-), MFR: powder feed rate (kg/h)].

228 respectively. However, as the fit between the experimental and predicted RTDs was poor,  
229 this model failed to represent the mixing properly resulting in an exceptionally low value of  
230  $n$  for all the runs (Fig 4). This situation arises when there are dead or stagnant pockets in  
231 the system along with the dispersion effects leading to a long tail in the RTD (Fogler, 2006).  
232 Therefore, for a further change in the model structure the conceptual model proposed by  
233 Kumar et al. (2008) including the  $p$  and  $d$  was used to define the RTD in the TSG (eq. 5).

### 234 *TIS with plug-flow volume fraction and dead-zones*

235 This model allowed estimation of the plug-flow volume fraction ( $p$ ) and degree of mixing  
236 in terms of a finite constantly stirred tank reactors ( $n$ ) having dead zones ( $d$ ) (Fig. 2). A  
237 significant improvement in the fit between the experimental and estimated RTD data was  
238 established by introducing the dead zones ( $d$ ) in the model structure (Fig. 5). The RSS  
239 for different runs varied from 5 to 60 and the  $R^2$  between 0.93 and 0.99, which is much  
240 better than observed for the other model structures. This also suggests that the TIS model  
241 with plug-flow volume fraction and dead zones is the most suitable to conceptually define  
242 RTD in the TSG and can flexibly reflect the behaviour of the system in the domain of the  
243 experiment. The obtained  $p$  values are found between 0.2–0.65, similar to the TIS model  
244 with plug-flow volume fraction only. The values of  $n$  and  $d$  ranged from 2 to 6 and from 0.01  
245 to 0.54, respectively. Due to a very good fit between the experimental and estimated RTD by  
246 this model, the calculated values for the parameters can be reliably used for characterisation  
247 of residence time and mixing in the TSG.

248 Therefore, based on the parameters estimated by this model, further detailed analysis  
249 of the twin-screw granulation system will be presented in the next section. A complete list  
250 of parameter sets, RSS and  $R^2$  values at different process conditions for all three model  
251 configurations is provided as supplementary data (Table S1).

### 252 *3.2. Analysis of RTD using TIS model with plug-flow and dead-volume fractions*

253 Prior to a comprehensive analysis of modeling results it is indispensable to know how  
254 reliable the parameter estimates are. Although only certain numerically estimated parameter  
255 combinations for the model could closely reproduce the experimental RTD of the process,

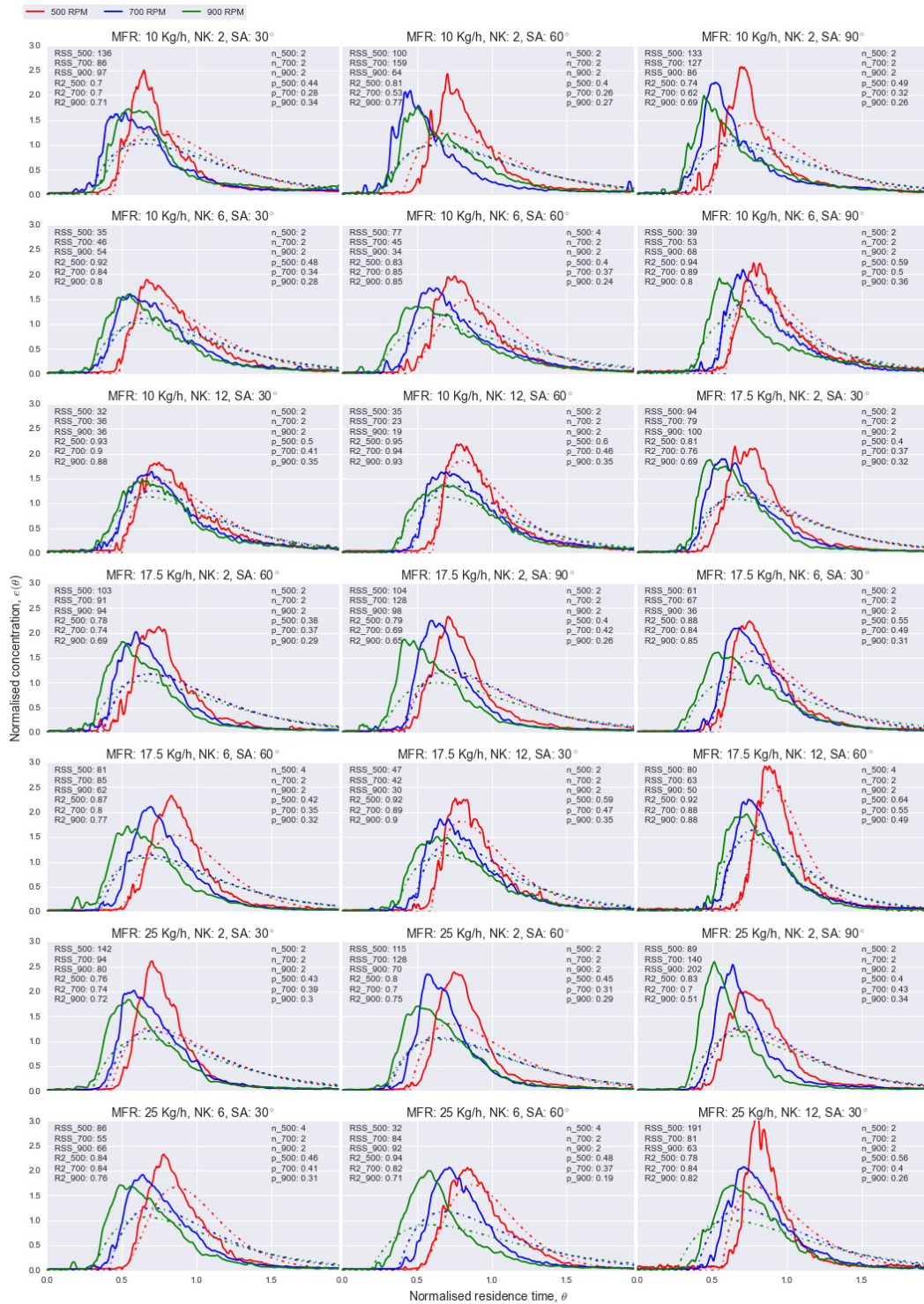


Figure 4: Experimental (—) vs. predicted (-.-) RTD by a TIS with plug-flow volume fraction model at different screw speed (500, 700, 900 RPM), powder feed rate (10-25 kg/h), number of kneading discs (2, 6, 12) and stagger angle (30-90°) [SA: stagger angle (°), NK: number of kneading discs (-), MFR: powder feed rate (kg/h)].

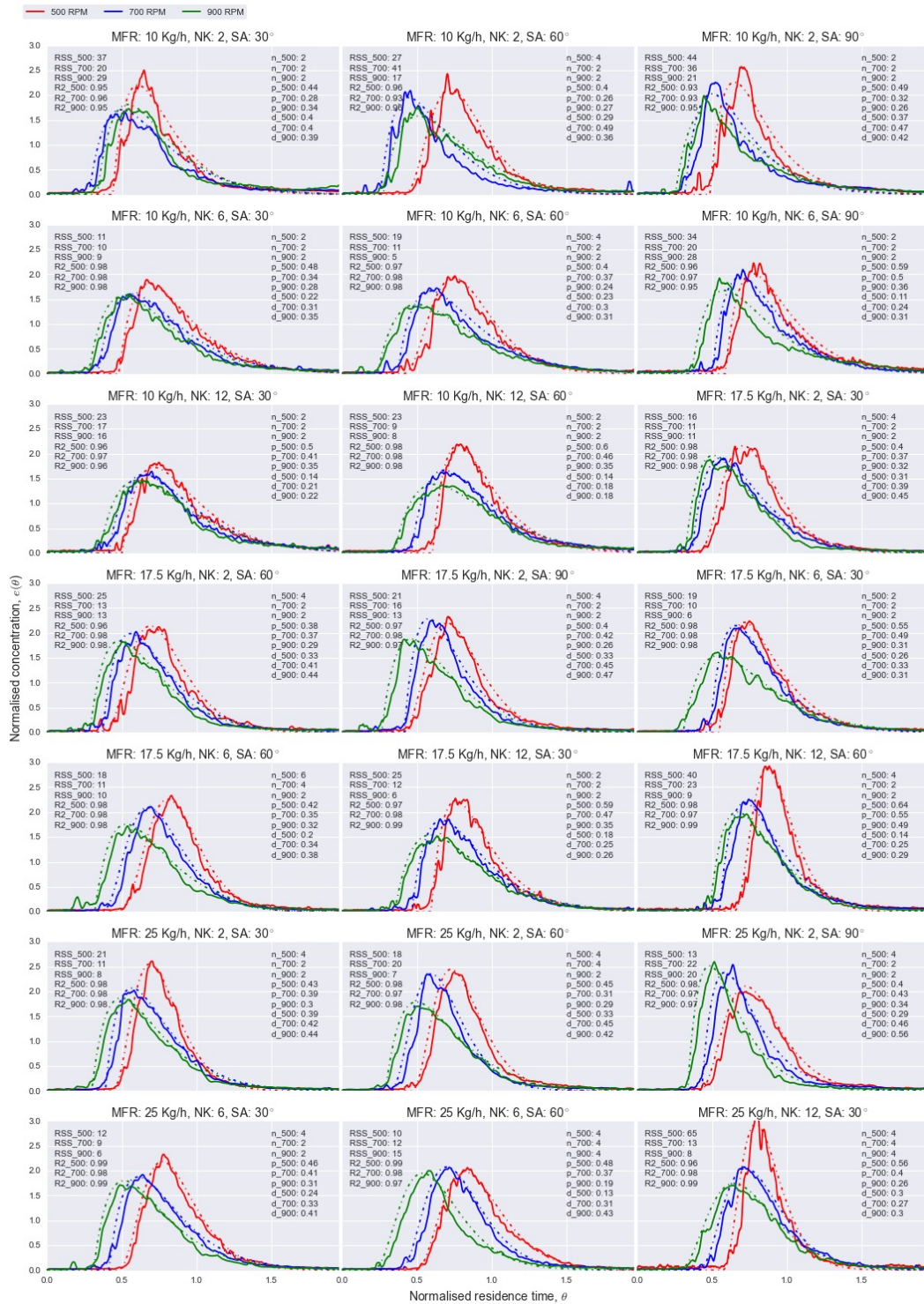


Figure 5: Experimental (—) vs. predicted (-.-) RTD by a TIS with plug-flow and dead-volume fractions model at different screw speed (500, 700, 900 RPM), powder feed rate (10-25 kg/h), number of kneading discs (2, 6, 12) and stagger angle (30-90°) [SA: stagger angle (°), NK: number of kneading discs (-), MFR: powder feed rate (kg/h)].

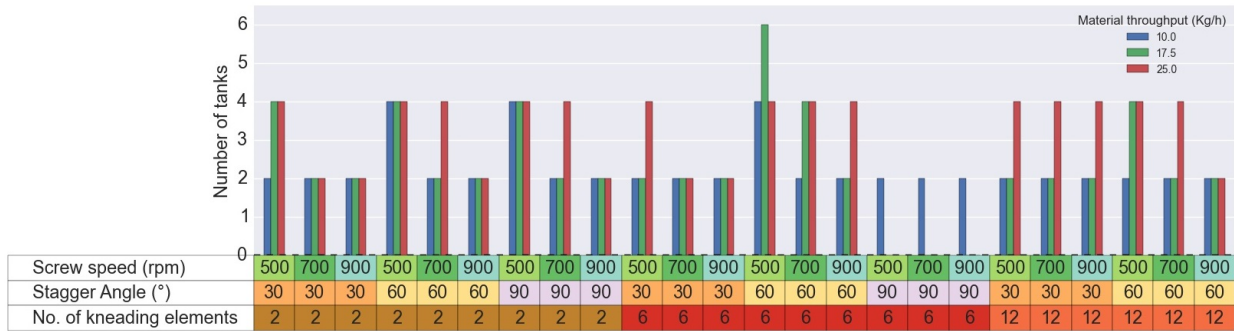


Figure 6: Effects of change in the process conditions on the plug-flow volume fraction as predicted by the TIS model with plug-flow volume fraction and dead zones.

256 ignoring the dependencies among the estimated parameters may lead to an identifiability  
 257 problem and meaningless estimates which severely reduces the prediction power of the model.  
 258 Therefore, practical identifiability was analysed globally over the complete parameter space  
 259 by the collinearity analysis. The collinearity index (eq. 6) was found to be 1.87, which is  
 260 sufficiently low to suggest that there was no significant interrelation between parameters.

### 261 3.2.1. Effect of process settings on plug-flow volume fraction in the TSG

262 The effect of powder feed rate (10-25 kg/h) on the plug-flow volume fraction ( $p$ ) was  
 263 very low for a lower number of kneading discs, however, for 6 and 12 kneading discs, the  
 264 plug-flow volume fraction increased with an increase in powder feed rate (Fig. 6). Similarly,  
 265 increasing the number of kneading discs caused an increase in the plug-flow volume fraction  
 266 in the TSG. Also, the effect of a change in stagger angle was less prominent for a low  
 267 number of kneading discs. However, for 6 and 12 kneading discs, the plug-flow volume  
 268 fraction increased significantly when stagger angle increased from 30° to 60° and then to  
 269 90°. The effect of screw speed was most dominant, and therefore, the plug-flow volume  
 270 fraction always reduced with the increase in the screw speed (500 to 700 and 900 rpm)  
 271 irrespective of other process settings.

272 These results suggest that kneading blocks in the TSG screws act like a plug-flow region  
 273 and the fill ratio in this region is critical. An increase in powder feed rate led to a high fill ratio  
 274 due to a higher material flux, whereas the increase in screw speed increased conveying rate



275 leading to reduction in the fill ratio. Since the  $p$  is the ratio between minimum residence time  
276 ( $t_{min}$ ) and mean residence time ( $\bar{t}$ ) (eq. 4), and since we know from a previous experimental  
277 study (Kumar et al., 2014b) that an increasing powder feed rate and screw speed cause a  
278 reduction in  $\bar{t}$ , it can be inferred that an increase in powder feed rate causes a relatively  
279 greater reduction in  $\bar{t}$  than  $t_{min}$  (narrowing of the RTD) and hence a higher  $p$ . However, when  
280 the screw speed was increased the relative reduction in  $t_{min}$  was greater than  $\bar{t}$  (broadening  
281 of the RTD), leading to a lower  $p$ . Hence, powder feed rate and screw speed, despite having  
282 the same effect on  $\bar{t}$ , have an opposite influence on the axial mixing.

### 283 3.2.2. Effect of process settings on axial mixing in the TSG

284 Mixing of the material within the shortest possible granulator length is of key importance  
285 in TSG. Beside the indirect measurement of axial mixing in terms of the ratio between  $t_{min}$   
286 and  $\bar{t}$ , in the TIS model with plug-flow volume fraction and dead zones the axial mixing is  
287 directly quantified in terms of the constantly stirred tank reactors ( $n$ ). The trend of change  
288 in  $n$  at various process settings suggests that the level of axial mixing was most dominantly  
289 controlled by the screw speed (Fig. 7). At a low screw speed (500 rpm), the value of  $n$  was  
290 mostly 4 compared to the experiments with a high screw speed (900 rpm) where it was 2.  
291 Also, a high powder feed rate along with a low screw speed, i.e., the high fill ratio condition,  
292 led to reduction in axial mixing. At a high powder feed rate, an increase in the number of  
293 kneading discs from 2 to 6 and then to 12 as well as a change of the stagger angle ( $30^\circ$   
294  $60^\circ$ ) also caused a reduction in the axial-mixing level despite a high screw speed (900 rpm),  
295 and the  $n$  increased to 4. The runs for  $90^\circ$  stagger angle could not be performed due to low  
296 axial mixing, which caused jamming of the granulator. However, an increase in the screw  
297 speed to its maximum (900 rpm) mostly resulted in resetting of the axial mixing to the same  
298 level ( $n = 2$ ).

299 These results suggest that powder feed rate and screw speed together dictate the axial  
300 mixing. Therefore, a balance between the throughput force and conveying rate is needed to  
301 obtain good axial mixing inside the TSG. At a high conveying rate, material throughput can  
302 be increased without loss in mixing, however, an increase beyond the conveying capacity of

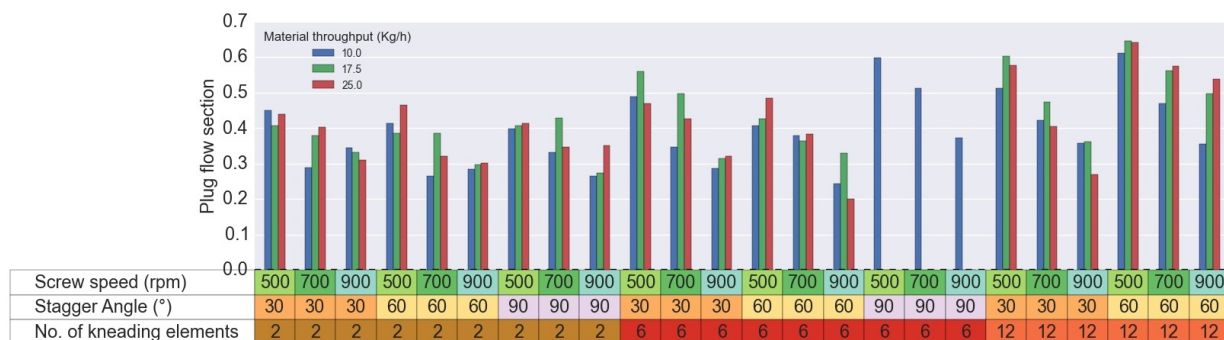


Figure 7: Effects of change in the process conditions on the number of TIS as predicted by the TIS model with plug-flow volume fraction and dead zones.

303 the screw may lead to a sudden change in flow regime to plug-flow and complete jamming  
 304 of the granulator (Kumar et al., 2014b).

### 305 3.2.3. Effect of process settings on dead zones in the TSG

306 Although axial mixing reflected by broadening of the RTD is necessary to compensate  
 307 for process variations (Kumar et al., 2014b), the excessive broadening in the tail region of  
 308 the RTD may also result from a stagnant region and excessive backing inside the TSG. Such  
 309 a desirable region may lead to build-up of material in long runs and is therefore estimated by  
 310 the dead zones ( $d$ ) in the model. The value of  $d$  was primarily influenced by the screw speed  
 311 and the number of kneading discs (Fig. 8). When the number of kneading discs increased  
 312 in the screw configuration,  $d$  decreased monotonically. Furthermore, an increase in screw  
 313 speed caused a reduction in  $d$ . In contrast, for a higher number of kneading discs (6 and 12),  
 314 an increase in powder feed rate caused an increase in  $d$ . This change is once again related  
 315 to the higher throughput force by the increased material flux.

316 These results indicate that the kneading blocks, which normally work under a more filled  
 317 channel condition than the transport screws, prevent excessive back-mixing in the TSG.  
 318 Also, increasing fill ratio reduces the stagnant region and consequently lowers the dead zone  
 319 inside the mixed flow section of the TSG. However, when the slippage rate increases due to  
 320 an increase in screw speed, there is a greater possibility of back-mixing, hence an increase  
 321 in  $d$ . Also, the conveying force helps in clearing the flow in the kneading blocks leading to

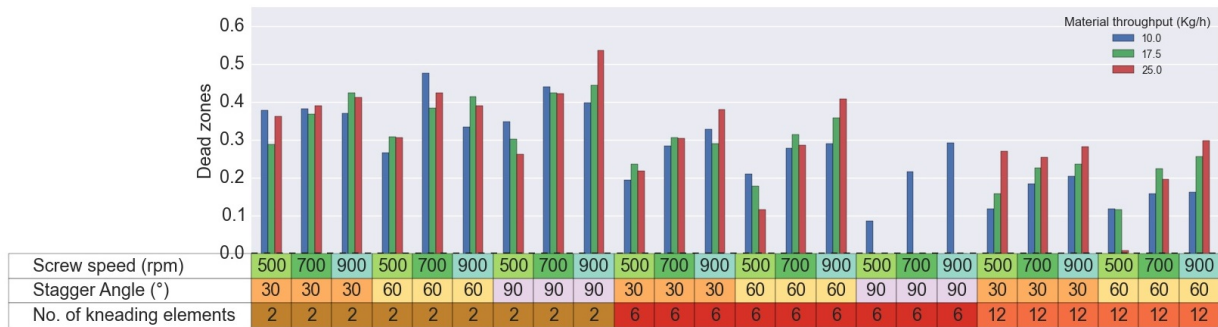


Figure 8: Effects of change in the process conditions on the dead-volume fractions inside the TSG barrel as predicted by the TIS model with plug-flow volume fraction and dead zones.

322 more back-mixing.

323 Beside the modelling and system identification owing to a good agreement between the  
 324 simulated and the experimental RTD data, this study also established that the combina-  
 325 tion of modelling and dedicated experimental data collection is very effective for gaining  
 326 an improved insight into the transport and mixing characteristics of material in the TSG.  
 327 Although the presented study is not "generic" to all formulations due to the likely differ-  
 328 ence in the granulation behaviour of different excipients (such as microcrystalline cellulose  
 329 and dibasic calcium phosphate), the method used in this study (both data collection and  
 330 modelling) is generic and can be repeated for other excipients. The knowledge gained from  
 331 this study can now be used as the basis for future extensive numerical simulation of flow  
 332 and transport in the TSG using Discrete Element Method (DEM). The, DEM requires enor-  
 333 mous numerical and computational effort due to the large number of equations, the strong  
 334 coupling between various physical processes and the difficulties to resolve boundaries of the  
 335 flow domain in the intermeshing twin-screw involved. However, these models are necessary  
 336 for complete understanding of the multiphase flow and mixing of wetted powder such as  
 337 local residence time and impact speed of colliding granules in the screw zones, which are  
 338 important for understanding the granulation mechanism in the TSG. Till an extensive DEM  
 339 model is developed, the best-fit conceptual model consisting of algebraic equation to describe  
 340 a plug flow in series with a finite number of constantly stirred tank reactors having dead  
 341 volume fractions can be applied for representation of the RTD in a TSG with a reasonable

342 accuracy along with simplicity and computational advantages.

#### 343 **4. Conclusions**

344 In this study, a systematic evaluation of the performance of three different conceptual  
345 models for the description of the residence time distribution in a twin-screw granulator has  
346 been performed. The suitability of the model framework was examined using the statistical  
347 difference between the experimental and estimated residence time distribution for runs with  
348 different screw configurations and process settings. The TIS model assuming plug-flow  
349 volume fraction in series with a finite constantly stirred tank reactors with dead zones was  
350 found to be the most suitable conceptual model for describing the experimentally measured  
351 residence time distribution in a twin-screw granulator. As estimated by this model, the  
352 kneading block in the screw configuration significantly stimulates the plug-flow transport  
353 of material inside the granulator. Furthermore, the results showed that mixing and dead  
354 zones are generally affected by the fill level inside the twin-screw granulator barrel, thus  
355 a good balance between the throughput force and the conveying rate is necessary for a  
356 good axial mixing and reduction in the stagnant regions inside the twin-screw granulator.  
357 The steady-state models consisting of algebraic equations rather than the physical models  
358 containing differential equations, achieve a reasonable accuracy in representation of the RTD  
359 along with the simplicity of implementation and computational advantages. Therefore, the  
360 conceptual TIS model describing RTD as a plug flow in series with a finite number of  
361 constantly stirred tank reactors having dead volume fractions was suggested for improved  
362 understanding the mixing and transport of material in the twin-screw granulator. Future  
363 experiments and modelling studies should investigate the effect of other formulations with  
364 significantly different raw material properties.

#### 365 **5. Acknowledgements**

366 Financial support for this research from the BOF (Bijzonder Onderzoeksfonds Univer-  
367 siteit Gent, Research Fund Ghent University) is gratefully acknowledged.

368 **List of symbols and abbreviations**

$\gamma$	collinearity index
$\sigma_{tm}^2$	variance
$d$	dead flow fraction
$e(\theta)$	normalised residence time
$n$	number of well mixed tank
$p$	plug-flow fraction
$\bar{t}$	mean residence time
$t_{min}$	minimum residence time
$R^2$	coefficient of determination
RSS	residual sum of the square
TIS	Tanks-in-series
RTD	residence time distribution
TSG	twin-screw granulation
$\tilde{S}$	normalised sensitivity matrix

## 369 References

- 370 Althaus, T. O., Windhab, E. J., Jan 2012. Characterization of wet powder flowability by shear cell mea-  
371 surements and compaction curves. *Powder Technol.* 215-216, 59–65.
- 372 Bakalis, S., Fryer, P. J., Parker, D. J., 2004. Measuring velocity distributions of viscous fluids using positron  
373 emission particle tracking (pept). *AIChE J.* 50 (7), 1606–1613.
- 374 Brun, R., Reichert, P., Künsch, H. R., 2001. Practical identifiability analysis of large environmental simula-  
375 tion models. *Water Resour. Res.* 37 (4), 1015–1030.
- 376 Dhenge, R. M., Cartwright, J. J., Hounslow, M. J., Salman, A. D., 2012. Twin screw granulation: Steps in  
377 granule growth. *Int. J. Pharm.* 438 (1-2), 20–32.
- 378 Dhenge, R. M., Fyles, R. S., Cartwright, J. J., Doughty, D. G., Hounslow, M. J., Salman, A. D., 2010.  
379 Twin screw wet granulation: Granule properties. *Chem. Eng. J.* 164 (2-3), 322–329, *Pharmaceutical*  
380 *Granulation and Processing*.
- 381 El Hagrasy, A., Hennenkamp, J., Burke, M., Cartwright, J., Litster, J., 2013. Twin screw wet granulation:  
382 Influence of formulation parameters on granule properties and growth behavior. *Powder Technol.* 238,  
383 108–115.
- 384 Fogler, H., 2006. *Elements Of Chemical Reaction Engineering*. Pearson international edition. Prentice Hall  
385 Professional Technical Reference.
- 386 Gao, Y., Muzzio, F. J., Ierapetritou, M. G., Sep. 2012. A review of the Residence Time Distribution (RTD)  
387 applications in solid unit operations. *Powder Technol.* 228, 416–423.
- 388 Kumar, A., Ganjyal, G. M., Jones, D. D., Hanna, M. A., 2008. Modeling residence time distribution in a  
389 twin-screw extruder as a series of ideal steady-state flow reactors. *Journal of Food Engineering* 84 (3),  
390 441 – 448.
- 391 Kumar, A., Gernaey, K. V., De Beer, T., Nopens, I., 2013a. Model-based analysis of high shear wet granula-  
392 tion from batch to continuous processes in pharmaceutical production – a critical review. *Eur. J. Pharm.*  
393 *Biopharm.* 85 (3, Part B), 814 – 832.
- 394 Kumar, A., Gernaey, K. V., De Beer, T., Nopens, I., 2013b. One dimensional model of the prediction of  
395 residence time distribution granulation in a twin-screw granulator. In: *6th International Granulation*  
396 *Workshop*.
- 397 Kumar, A., Vercruyssen, J., Bellandi, G., Gernaey, K. V., Vervaet, C., Remon, J. P., Beer, T. D., Nopens,  
398 I., 2014a. Experimental investigation of granule size and shape dynamics in twin-screw granulation.  
399 *International Journal of Pharmaceutics* 475 (1-2), 485 – 495.
- 400 Kumar, A., Vercruyssen, J., Toiviainen, M., Panouillot, P.-E., Juuti, M., Vanhoorne, V., Vervaet, C., Remon,  
401 J. P., Gernaey, K. V., Beer, T. D., et al., 2014b. Mixing and transport during pharmaceutical twin-screw  
402 wet granulation: experimental analysis via chemical imaging. *Eur. J. Pharm. Biopharm.* 87 (2), 279 –

403 289.

404 Lee, K. T., 2013. Continuous granulation of pharmaceutical powder using a twin screw granulator. Ph.D.  
405 thesis, University of Birmingham.

406 Lee, K. T., Ingram, A., Rowson, N. A., Aug. 2012. Twin screw wet granulation: the study of a continuous  
407 twin screw granulator using Positron Emission Particle Tracking (PEPT) technique. *Eur. J. Pharm.*  
408 *Biopharm.* 81 (3), 666–73.

409 Levenspiel, O., 1999. *Chemical Reaction Engineering*, 3rd Edition. John Wiley & Sons.

410 Nelder, J. A., Mead, R., 1965. A simplex method for function minimization. *Comput. J.* 7 (4), 308–313.

411 Oliphant, T. E., 2007. Python for scientific computing. *Comp. Sci. Eng.* 9 (3), 10–20.

412 Puaux, J., Bozga, G., Ainsler, A., 2000. Residence time distribution in a corotating twin-screw extruder.  
413 *Chemical Engineering Science* 55 (9), 1641 – 1651.

414 Vercruyssen, J., Córdoba Díaz, D., Peeters, E., Fonteyne, M., Delaet, U., Van Assche, I., De Beer, T., Remon,  
415 J. P., Vervaet, C., 2012. Continuous twin screw granulation: Influence of process variables on granule and  
416 tablet quality. *Eur. J. Pharm. Biopharm.* 82 (1), 205–211.

417 Vercruyssen, J., Toiviainen, M., Fonteyne, M., Helkimo, N., Ketolainen, J., Juuti, M., Delaet, U., Assche,  
418 I. V., Remon, J. P., Vervaet, C., De Beer, T., 2013. Visualization and understanding of the granulation  
419 liquid mixing and distribution during continuous twin screw granulation using NIR chemical imaging.  
420 *Eur. J. Pharm. Biopharm.* 86 (3), 383–392.